Finite-difference modeling experiments for seismic interferometry

Jan Thorbecke* and Deyan Draganov †, Delft University of Technology, Department of Geotechnology, Section of Applied Geophysics, The Netherlands

SUMMARY

In passive seismic interferometry data are measured with (highly sensitive) geophones over a long period of time. The measured signals can be correlated with each other to retrieve reflection data. The quality of the retrieved reflection data is, among others, dependent on the number of passive sources measured during the recording time, the source strength, and the source distribution. To investigate these dependency relations, controlled modeling studies have to be carried out. We wrote a 2D visco-elastic and visco-acoustic finite-difference code and specially designed it for the simulation of long-time passive seismic measurements. Based on a first series of modeling experiments, we observed that the position of the passive sources and the length of the source signals are of direct influence on the quality of the retrieved reflections.

Introduction

The retrieval of surface waves using natural sources has already led to numerous successful studies (Campillo and Paul, 2003). Seismic Interferometry used for the retrieval of reflection data (body waves) has been successfully applied only recently (Draganov et al., 2007, 2009). However, in many cases it remains difficult to interpret the retrieved wavefields and verification with modeled data is useful.

Within our group of Applied Geophysics, research in Seismic interferometry (SI) for the retrieval of body waves plays a central role (Wapenaar and Fokkema, 2006). To test ideas and new concepts passive measurements are needed. Unfortunately, passive measurements, which can be used to study SI, are still rare and difficult to obtain. For the moment we have to rely on forward modeling of passive measurement to gain experience in the practical use of SI. The standard data-modeling tools are not very suitable to model passive measurements and new modeling tools have to be developed. A forward-modeling program has been written to model realistic SI measurements. The goal of modeling studies is to get a better understanding of what influences the quality of the retrieved reflections. In using modeling experiments we hope to find answers to the following questions:

- how much data need to be recorded for a satisfactory reflection retrieval;
- how many measurement stations are needed;
- how many passive sources should be captured during the recording time;
- the influence of source amplitudes;
- and what is the influence of attenuation.

Theory

In the brief theoretical background given in this section, we follow Wapenaar and Fokkema (2006) and derive SI from reciprocity theory. Consider a Green's function $G(\mathbf{x},\mathbf{x}_A,t)$ for an inhomogeneous lossless acoustic medium, where $\mathbf{x}$ and $\mathbf{x}_A$ are the Cartesian coordinate vectors for the observation and source points, respectively, and where t denotes time. We define the temporal Fourier transform as $\hat{G}(\mathbf{x},\mathbf{x}_A,\omega) = \int_{-\infty}^{\infty}\exp(-j\omega t)G(\mathbf{x},\mathbf{x}_A,t)\mathrm{d}t$, where j is the imaginary unit and ω the angular frequency. Assuming the unit point source at $\mathbf{x}_A$ is of the volume injection-rate type, the wave equation for $\hat{G}(\mathbf{x},\mathbf{x}_A,\omega)$ reads

$$\rho\partial_i(\rho^{-1}\partial_i\hat{G}(\mathbf{x},\mathbf{x}_A)) + (\omega^2/c^2)\hat{G}(\mathbf{x},\mathbf{x}_A) = -j\omega\rho\delta(\mathbf{x}-\mathbf{x}_A). \quad (1)$$

Here $c = c(\mathbf{x})$ and $\rho = \rho(\mathbf{x})$ are the propagation velocity and mass density of the inhomogeneous medium and ∂_i denotes the partial derivative in the x_i-direction (Einstein's summation convention applies to repeated subscripts). The representation of $\hat{G}$, as derived for seismic interferometry from Rayleigh's reciprocity theorem (Rayleigh, 1878; Wapenaar et al., 2004; Wapenaar, 2004; Wapenaar et al., 2005), reads

$$\hat{G}_h(\mathbf{x}_A,\mathbf{x}_B) = \oint_{\partial\mathbb{D}} \frac{-1}{j\omega\rho(\mathbf{x})}\Big(\hat{G}^*(\mathbf{x}_A,\mathbf{x})\partial_i\hat{G}(\mathbf{x}_B,\mathbf{x}) \quad (2)$$

$$-\big(\partial_i\hat{G}^*(\mathbf{x}_A,\mathbf{x})\big)\hat{G}(\mathbf{x}_B,\mathbf{x})\Big)n_i\mathrm{d}^2\mathbf{x}, \quad (3)$$

with

$$\hat{G}_h(\mathbf{x}_A,\mathbf{x}_B) \hat{=} \hat{G}(\mathbf{x}_A,\mathbf{x}_B) + \hat{G}^*(\mathbf{x}_A,\mathbf{x}_B) = 2\Re\{\hat{G}(\mathbf{x}_A,\mathbf{x}_B)\}, \quad (4)$$

where $\partial\mathbb{D}$ is an arbitrary closed surface with outward pointing normal vector $\mathbf{n} = (n_1,n_2,n_3)$ and the asterisk denotes complex conjugation.

When we assume that the sources are uncorrelated (both in space and in time) we can write the observed wavefields as

$$\hat{p}^{obs}(\mathbf{x}_A) = \oint_{\partial\mathbb{D}} \hat{G}(\mathbf{x}_A,\mathbf{x})\hat{N}(\mathbf{x})\mathrm{d}^2\mathbf{x} \quad \text{and} \quad (5)$$

$$\hat{p}^{obs}(\mathbf{x}_B) = \oint_{\partial\mathbb{D}} \hat{G}(\mathbf{x}_B,\mathbf{x})\hat{N}(\mathbf{x})\mathrm{d}^2\mathbf{x},$$

where the noise signal $\hat{N}(\mathbf{x},\omega)$ has to fulfill

$$\langle\hat{N}(\mathbf{x})\hat{N}^*(\mathbf{x}')\rangle = \delta(\mathbf{x}-\mathbf{x}')\hat{S}(\omega), \quad (6)$$

$\langle.\rangle$ a spatial ensemble average, and $\hat{S}(\omega)$ the power spectrum of the noise sources, equation 5 reduces to

$$2\Re\{\hat{G}(\mathbf{x}_A,\mathbf{x}_B)\}\hat{S}(\omega) \approx \frac{2}{c\rho}\langle\hat{p}^{obs*}(\mathbf{x}_A)\hat{p}^{obs}(\mathbf{x}_B)\rangle. \quad (7)$$

Equation 7 and 5 are used in the remainder of this paper to retrieve reflection data from modeled data representing passive seismic measurements ($\hat{p}^{obs}$).

Modeling experiments

To simulate passive seismic measurements we have chosen to use a 2-dimensional finite-difference approach based on the work of Virieux (1986) and Robertsson et al. (1994). The main reason for choosing the finite-difference method is that it runs efficiently on standard X86 and multi-core hardware (including graphical card's). For the moment, only the 2-dimensional case is implemented to gain experience and be able to run experiments within a reasonable compute time. An extension to three dimensions will be carried out in the near future. For reading input parameters and access to files on disk use is made of the Seismic Unix (SU) parameter interface and segy-based data file format. In the code, four different schemes are implemented: acoustic, visco-acoustic, elastic, and visco-elastic. We will not go into all the implementation details and only explain the aspects which are related to the modeling of measurements which can be used for SI. Details about the use of the program can be found in a separate manual distributed with the code. In the remainder of this section the implementation of noise signature sources is explained.

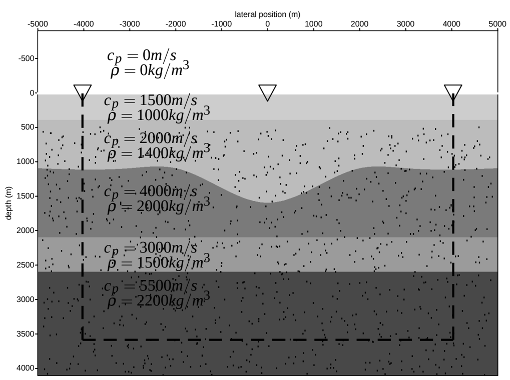

Figure 1: Noise sources are positioned at random locations, visible as small black dots, within the model. At $z = 0$ a free surface is implemented and the receivers are placed on it. The $\bigtriangledown$ indicate the receiver positions, which are placed at level $z = 0$.

As a first SI experiment with noise sources, we use the model shown in Figure 1, with random source positions below $z =$ 500 m. In the figure, the source positions, in total 1000, are shown as tiny black dots. The receivers are placed on the free surface at $z = 0$ on a 10 m grid covering the whole surface. For the investigation of the sources' influence on the retrieved result the source signal duration, and start time is varied. The source signature is a random sequence with a maximum frequency of 30 Hz. The finite-difference program simulates all the 1000 sources within only one run of the program. This makes the modeling very efficient and allows to model many different experiments within a reasonable computational time.

Figure 2a shows the reference result: a shot record for a virtual source position in the middle of the model. Figures 2b to 2f show SI results using a total recording time of 120 seconds and a maximum frequency of 30 Hz. The source-signature duration is varying from a maximum of 120 s (Figure 2b) to a maximum of 5 s (Figure 2f). The sources are started at a random time in the time interval of 0-120 s and during the

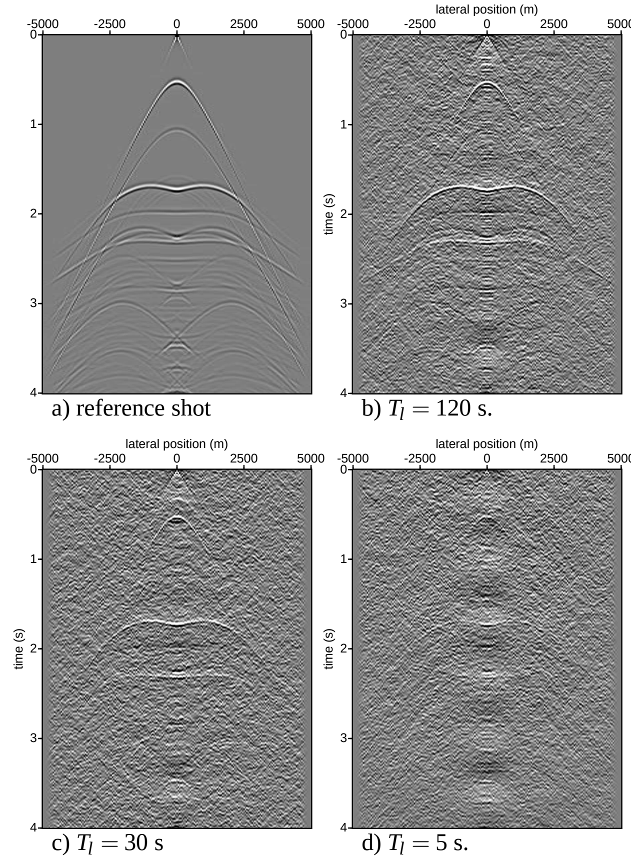

Figure 2: a) A directly modeled reference result. Retrieved results using different maximum source-signature lengths (T_l): b) 120 , c) 30 , and d) 5 s. To retrieve the SI result noise signatures with a maximum frequency of 30 Hz are used, 1000 sources at random positions, a random start time between 0 and 120 s and a total recording time of 120 s.

modeling many sources are active simultaneously. It is clear that longer source signatures give a better retrieval of the reflections. Note also that only the strongest reflections in the model are visible through the noise and the free-surface and internal multiples are not clearly visible. In most cases it is not known how long passive sources are active in the subsurface. It is expected that from a S/N perspective more sources with a short signal duration would give similar results to fewer sources with a longer duration length. This would also mean that using longer passive measurements, more (short- and/or long-duration) passive sources are captured and a better retrieval can be made. In seismically active areas maybe a few days of recoding would be sufficient, while in more quiet areas on the earth a few months would be needed.

In Figure 3 the average signature duration is kept constant (with a maximum length of 120 seconds), but the number of sources is varied. We can see that the more randomly distributed sources are present, the better the retrieved result. Above a certain number of sources (in the example around 500) the strongest reflection events are constructed correctly, meaning that the stationary-phase area for those reflections is sampled densely enough. Adding more sources helps to retrieve other reflection information which have a smaller stationary region. For example Figure 3a, which is constructed using 8000 sources, show the bow-tie shaped event starting at 3.0 s more clearly than 3b with only 1000 sources.

Recording the contribution of more sources does not improve the S/N ratio for the already correctly retrieved reflections. Figure 3f shows a comparison of the middle traces. The traces are normalized to the maximum value per trace (around $t = 1.75$), note that the most left trace (8000 sources) has the best retrieval, but there is no S/N improvement, of the first strong reflection event, compared to the last trace (50 sources). This is in contrast with NMO stacking, which improves the S/N ratio by a factor $\sqrt{N}$, where N is the number of traces stacked. There are two possible explanations for this observation: In the used modeling example the sources are not placed on a nice smooth surface, as is required by the theory, but are distributed in a volume below 500 m depth. Integration over this volume of sources will also generate a lot of artifacts due to truncation effects. Even if the sources were nicely distributed along an ideal boundary surface $\partial\mathbb{D}_1$, when the Fresnel zone is sufficiently sampled by a certain number of sources (at least two sources per wavelength), adding more sources will not add extra information, since the constructive interference in the Fresnel zone constructs the physical amplitude.

In Figure 3, all the observed background noise is a result from the correlation, i.e., it is correlation noise. In field measurements there is also a random noise from the measurement equipment and the signal-to-random noise level would improve when more sources are contributing to the retrieved reflections.

To validate the explanations of the observed noise in Figure 3, the origin of the noise is further investigated. Is this noise caused by the noisy source signals, by the random positions of the sources or by a combination of both? This is tested with new experiments. Figure 4 shows the recorded data for three different kinds of source distributions and different source signatures. The used source distributions are;

- random positions between $500 \leq z \leq 4100$ m,
- random positions between $2700 \leq z \leq 4100$ m,
- and a horizontal plane at $z = 2700$ m with regularly spaced sources, just below the deepest reflector.

For the random source positions, 8000 sources are used, while for the sources positioned on the horizontal plane (Figure 4c and 4f) a source is placed on every grid point in the model (981 sources). Two types of source signatures are used: a Ricker wavelet with a frequency peak at 10 Hz (with a maximum frequency around 30 Hz) and uncorrelated random source signals (different at each source position) with a maximum frequency of 30 Hz.

The retrieved reflection responses of the recordings from Figure 4 are shown in Figure 5. The cleanest retrieval, i.e., the lowest level of the correlation noise, is given by the plane-wave response with a Ricker wavelet shown in Figure 5f, but this is also the poorest retrieval of reflection data. The correlation condition in equation(6) is not satisfied: both the source signature and source position are strongly correlated. The retrieved reflections using uncorrelated noise signatures, but a correlated source depth position at the horizontal plane $z = 2700$ is shown in Figure 5c. The retrieval is quite good and very similar to Figure 5b, where random source position are used below $z = 2700$ m. From these three experiments it can already be concluded that uncorrelated source signals are important for the quality of the retrieved reflections. Figure 5d and e use the same fixed (for all source positions) Ricker source signature, but have uncorrelated source positions. The retrieved reflection events are now clearly visible and the introduced noise is caused by the incomplete destructive interference outside the Fresnel zone. Note, that the results with the Ricker wavelet using a random start time and source position are in fact shot records which are uncorrelated (in time), because of the short signature of the Ricker wavelet.

The retrieval using noise signatures at random positions is shown in Figure 5a and b and similar reflection events and noise behavior is observed as in Figure 5c. A close examination of Figure 5a, where a volume of sources is used $500 \leq z \leq 4100$ m, shows that higher angles are retrieved better compared with Figure 5b. However, there are also ghost events introduced (indicated) (Thorbecke and Wapenaar, 2008).

In the examples of Figure 5 the sources are originating from a volume. Using SI theory which is based on a surface integral, those volume-distributed sources can be thought of to be located on a very complicated (irregular) surface which connects all the points together. The addition of this complex surface will not give one nice stationary contribution, which is the case for a regular/smooth surface. Another effect of this complex surface is that the normal to the surface will not coincide with the dipole source radiation pattern and the assumptions made for SI equation 7 (approximate dipoles by scaled monopoles) are not satisfied anymore. The observed ghost events in Figure 5a can also be explained by this complex integration surface and not satisfying the assumptions used in the derivation of equation 7.

Conclusions

Using our modeling program for passive seismic measurements we have carried out a few simple experiments. Although one has to be careful to draw conclusions from them, we have seen that a longer time duration of the passive source signal gives a better retrieval than short time signals. Non-transient passive sources would therefore be ideal for the retrieval of reflection data.

Much more experimental work is needed to formulate general statements what influences the quality of retrieved reflections. We hope that by making the modeling software freely available, other groups can also benefit from our efforts and gain more insight in the practical issues of SI.

Acknowledgements

We are thankful to research school ISES and StatoilHydro for supporting this research.

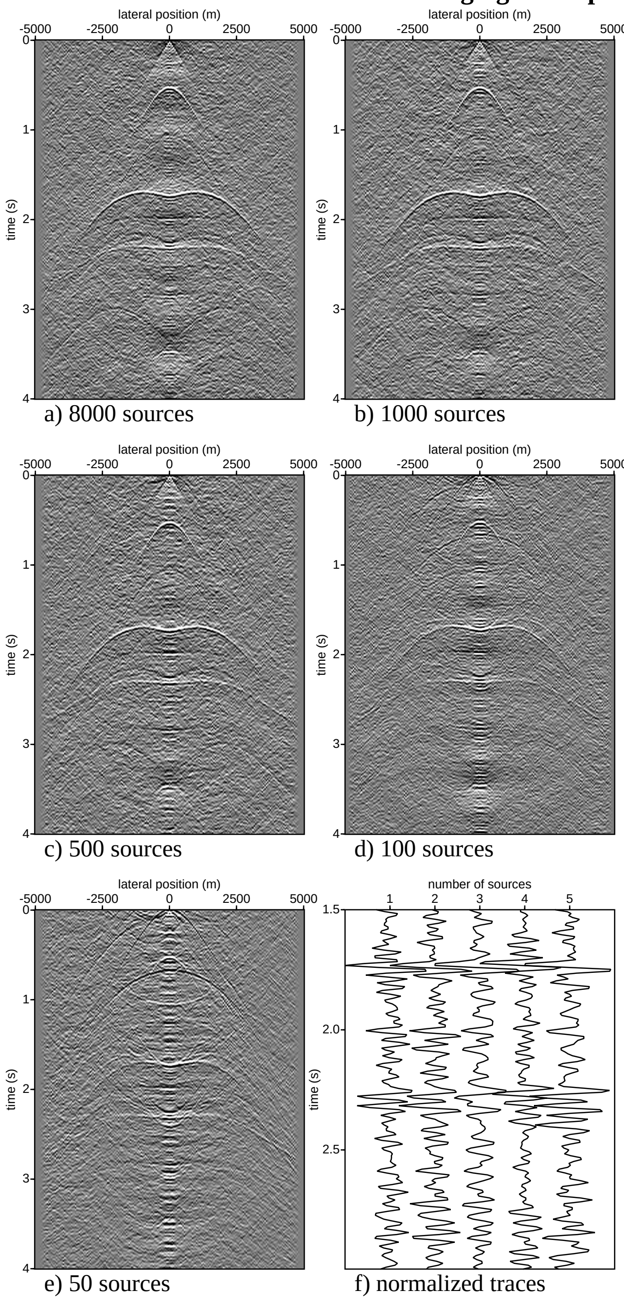

Figure 3: Seismic interferometry results for a varying number of sources. The sources have a random position in the model (see Figure 1) below $z = 500$ m. The used noise signatures have a maximum frequency of 30 Hz, a length between 0 and 120 s, and start at a random time between 0 and 120 s. The average noise-source duration is 60 s and the total recording time is 120 s. The total number of the noise sources is a) 8000, b) 1000, c) 500, d) 100 and e) 50. f) a comparison of the middle traces of a(trace number 1) until e(trace number 5) respectively.

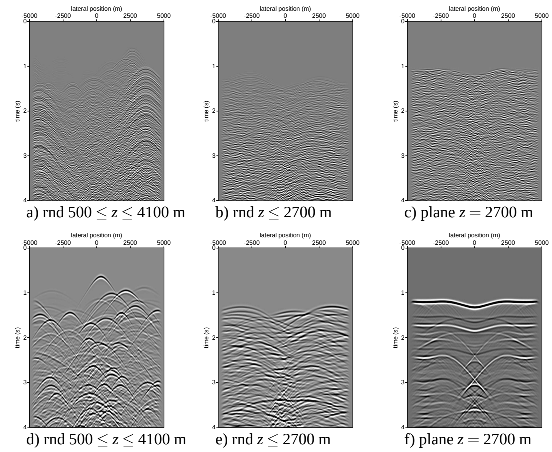

Figure 4: The first four seconds of modeled recordings at the surface that are used as the input for the seismic interferometry. The subsurface sources are distributed along all x-positions in the z-range indicated in the caption below the pictures. Noise signatures (every source has an unique signature) are used in a,b and c and the same Ricker wavelet is used in figures d,e and f. Note that the sources in c) and f) are started simultaneously. The abbreviation 'rnd' stands for random positions.

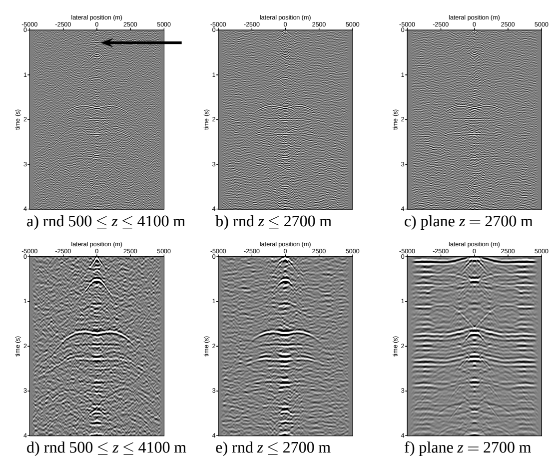

Figure 5: Retrieved results from the application of seismic interferometry when the inputs are recorded signals as shown in the corresponding panels in Figure 4. The arrow indicates a ghost event introduced by the type of source distribution.

REFERENCES

Campillo, M. and A. Paul, 2003, Long-range correlations in the diffuse seismic coda: Science, **299**, 547–549.

Draganov, D., K. Wapenaar, W. Mulder, J. Singer, and A. Verdel, 2007, Retrieval of reflections from seismic background-noise measurements: Geophysical Research Letters, **34**, L04305–1–L04305–4.

Draganov, D., X. Campman, J. Thorbecke, A. Verdel and K. Wapenaar, 2009, Reflection images from ambient seismic noise: Geophysics, **74**, A63–A67.

Rayleigh, J. W. S., 1878, The theory of sound. Volume II: Dover Publications, Inc. (Reprint 1945).

Robertsson, J. O. A., Blanch, J. O., and Symes, W. W., 1994, Viscoelastic finite-difference modeling: Geophysics, **59**, 1444–1456.

Thorbecke, J. and K. Wapenaar, Analysis of spurious events in seismic interferometry: 78th Annual International Meeting, SEG, Expanded Abstracts, PSC 1.1

Virieux, J., 1986. P-Sv wave propagation in heterogeneous media - Velocity-stress finite-difference method: Geophysics, **51**, 889–901.

Wapenaar, K., J. Thorbecke, and D. Draganov, , 2004, Relations between reflection and transmission responses of 3-D inhomogeneous media: Geophysical Journal International, **156**, 179–194.

Wapenaar, K., J. Fokkema, and R. Snieder, 2005, Retrieving the Green's function in an open system by cross-correlation: a comparison of approaches (L): Journal of the Acoustical Society of America, **118**, 2783–2786.

Wapenaar, K., 2004, Retrieving the elastodynamic Green's function of an arbitrary inhomogeneous medium by cross correlation: Physical Review Letters, **93**, 254301–1–254301–4.

Wapenaar, K., and J. Fokkema, 2006, Green's function representations for seismic interferometry: Geophysics, **71**, SI33–SI46.

EDITED REFERENCES

Note: This reference list is a copy-edited version of the reference list submitted by the author. Reference lists for the 2010 SEG Technical Program Expanded Abstracts have been copy edited so that references provided with the online metadata for each paper will achieve a high degree of linking to cited sources that appear on the Web.

REFERENCES

Campillo, M., and A. Paul, 2003, Long-range correlations in the diffuse seismic coda: Science, **299**, no. 5606, 547–549, doi:10.1126/science.1078551. PubMed

Draganov, D., K. Wapenaar, W. Mulder, J. Singer, and A. Verdel, 2007, Retrieval of reflections from seismic background-noise measurements: Geophysical Research Letters, **34**, no. 4, L04305doi:10.1029/2006GL028735.

Draganov, D., X. Campman, J. Thorbecke, A. Verdel, and K. Wapenaar, 2009, Reflection images from ambient seismic noise: Geophysics, **74**, no. 5, A63–A67, doi:10.1190/1.3193529.

Rayleigh, J. W. S., 1878, The theory of sound, Volume II: Dover Publications, Inc. (Reprint 1945).

Robertsson, J. O. A., J. O. Blanch, and W. W. Symes, 1994, Viscoelastic finite-difference modeling: Geophysics, **59**, 1444–1456, doi:10.1190/1.1443701.

Thorbecke, J., and K. Wapenaar, Analysis of spurious events in seismic interferometry: 78th Annual International Meeting, SEG, Expanded Abstracts, PSC 1.1

Virieux, J., 1986, P-Sv wave propagation in heterogeneous media - Velocity-stress finite-difference method: Geophysics, **51**, 889–901, doi:10.1190/1.1442147.

Wapenaar, K., J. Thorbecke, and D. Draganov, 2004, Relations between reflection and transmission responses of three-dimensional inhomogeneous media: Geophysical Journal International, **156**, 179–194. doi:10.1111/j.1365-246X.2003.02152.x

Wapenaar, K., J. Fokkema, and R. Snieder, 2005, Retrieving the Green's function in an open system by cross-correlation: a comparison of approaches: The Journal of the Acoustical Society of America, **118**, no. 5, 2783–2786, doi:10.1121/1.2046847.

Wapenaar, K., 2004, Retrieving the elastodynamic Green's function of an arbitrary inhomogeneous medium by cross correlation: Physical Review Letters, **93**, no. 25, 254301, doi:10.1103/PhysRevLett.93.254301. PubMed

Wapenaar, K., and J. Fokkema, 2006, Green's function representations for seismic interferometry: Geophysics, **71**, no. 4, SI33–SI46, doi:10.1190/1.2213955.